Description and Ultrasound Targeting of the Origin of the Suprascapular Nerve

P. LAUMONERIE,[1,2]* F. LAPÈGUE,[3] E. CHANTALAT,[2] N. SANS,[3] P. MANSAT,[1] AND M. FARUCH[3]

[1]Department of Orthopedics, Hôpital Pierre-Paul Riquet, Toulouse 31059, France
[2]Anatomy Laboratory, Faculty of Medicine, Toulouse 31062, France
[3]Department of Radiology, Hôpital Pierre-Paul Riquet, Toulouse 31059, France

Anatomical variations in the suprascapular nerve (SSN) and its depth in the suprascapular notch can make it difficult to target with ultrasonography (US). One alternative could be a proximal approach to the SSN, if US provides a reliable description of its origin (orSSN). The primary objective of this study was to demonstrate that US can reliably locate the orSSN. The secondary objective was to describe the features of the proximal SSN. Seventy brachial plexuses (BPs) from 30 healthy volunteers (60 BPs) and 5 cadavers (10 BPs) were included. There were two parts to this study: (1) description of the proximal SSN in healthy volunteers using US to determine the diameter, depth and location of the orSSN; (2) targeting of the orSSN with US in cadaver limbs to determine its distance from the needle, ink marking and locating the orSSN. In Part I, the diameter of the orSSN averaged 1.33 mm (1–9 mm) and its depth averaged 5.12 mm (2.7–10.6 mm). The orSSN was located in the upper trunk of the BP (53) or its posterior division (7). In Part II, the orSSN was successfully targeted in nine of the 10 specimens by US; the needle/orSSN distance averaged 3.8 mm (0–8 mm). The implanted needle was at the orSSN in two cases, proximal to it in seven and distal to it in one. US is a valid modality for describing and pinpointing the orSSN, irrespective of patient morphology. Clin. Anat. 30:747–752, 2017.

Key words: suprascapular nerve; brachial plexus; ultrasound

INTRODUCTION

The exact origin of the suprascapular nerve (SSN) has been the subject of controversy for over 400 years (Vesalius, 1555). According to published studies, it emerges from the upper trunk of the brachial plexus (UTBP) (Kerr, 1918; Leung et al., 2015), the bifurcation point (e.g., equivalent trifurcation) (Hanna, 2016), or a branch of the posterior division of the UTBP (Arad et al., 2014). According to Hanna (2016), the configuration of the branches of the UTBP can be summarized by the acronym SPA: suprascapular nerve (S), posterior division of the upper trunk (P), and anterior division of the upper trunk (A).

Magnetic resonance imaging (MRI) is the gold standard for describing the BP and its terminal branches (Boykin et al., 2010; Chalian et al., 2011; Ahlawat et al., 2015; Marquez Neto et al., 2016; Wang et al., 2016). During the last two decades, ultrasonography (US) of the suprascapular portion of the SSN has gained prominence for the dynamic exploration of neuropathies and for ultrasound-guiding of anesthetic nerve blocks in cases of acute and chronic shoulder pain (Karataş et al., 2002; Boykin et al., 2010; Chan et al., 2011; Stein et al., 2012; Bharti et al., 2015;

*Correspondence to: Pierre Laumonerie, Department of Orthope-dics, Hôpital Pierre-Paul Riquet, Place du Docteur Baylac, Toulouse 31059, France. E-mail: laumonerie.pierre@hotmail.fr

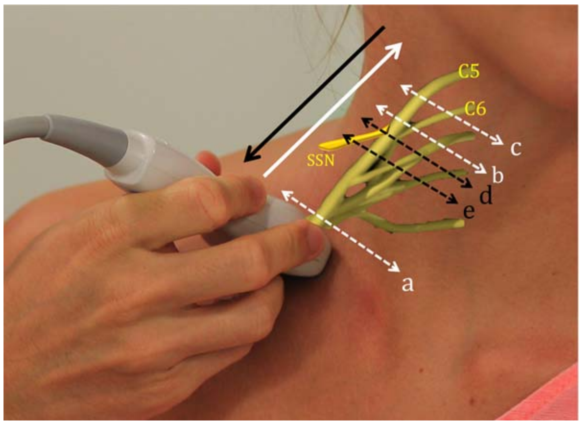

Fig. 1. Drawing of the US ski lift technique for exploring the BP. The US study of the supraclavicular portion of the BP (in yellow) was done on horizontal slices; the probe was translated upwards (white arrow) and then downwards (black arrow). This allowed us to explore fascicles outside the subclavian artery (SA) and above the clavicle **(a)**, spinal roots and trunks **(b)** at the level of the interscalene triangle **(b)**, and the origin of the roots in contact with the transverse processes **(c)**. In the downward direction, the upper trunk (UT) **(d)** distal to the interscalene triangle and then the origin of the SSN **(e)** were located successively. [Color figure can be viewed at wileyonlinelibrary.com]

Lewis et al., 2015; Chang et al., 2016; Dhir et al., 2016). The trajectory of the SSN at the level of the suprascapular notch is deep, inconsistent and in the vicinity of the suprascapular artery; these factors make ultrasound-guided procedures more challenging (Harmon and Hearty, 2007; Vorster et al., 2008; Siegenthaler et al., 2012; Battaglia et al., 2014). One alternative could be a proximal approach to the SSN, if US provides a reliable description of it.

The primary objective of this study was to show that the US “ski lift” technique can be applied to the BP to target the SSN’s origin (orSSN) (Lapegue et al., 2014). The primary hypothesis was that US can be used to pinpoint the orSSN. The secondary objective was to describe the features of the proximal portion of the SSN. The secondary hypothesis was that the supraclavicular course of the proximal SSN is superficial.

MATERIALS AND METHODS

Materials

Seventy BPs from 30 healthy volunteers (60 BPs) and five cadavers (10 BPs) were included.

The mean age of the healthy volunteers (12 men, 18 women) was 33.4 years (25 56 years); their mean body mass index (BMI) was 22.53 kg/m^2 (range, 17.63 32.87 kg/m^2). The mean age of the five fresh cadavers (two men, three women) (stored at 4°C) was 72.2 years (59 85 years) with a mean BMI of 23.8 kg/m^2 (range, 17 30 kg/m^2). A BP was excluded if there was a history of radiation therapy, surgery or trauma in the cervical, supraclavicular or shoulder girdle area. None of the specimens were excluded.

Methods

US exploration of the trajectory of the proximal SSN in the supraclavicular region was divided into two parts. In part I, the proximal portion of the SSN was described using US in healthy volunteers after securing institutional review board approval (CERNI-Université fédérale de Toulouse-2016 020). In part II, the accuracy with which the SSN was located using US was determined in cadaver limbs.

Description of Proximal SSN in Healthy Volunteers

The 30 healthy volunteers included in this portion of the study allowed us to describe the supraclavicular trajectory of 60 SSNs. For the exploration, a 14 18 MHz probe (Aplio 500, Toshiba®, San Jose, CA, United States) was used by a musculoskeletal radiologist with 18 years’ experience in peripheral nerve imaging (F.L.).

The US protocol was defined beforehand and used with each BP; this is the “ski lift” method previously described by Lapegue et al. (2014) (Figs. 1 and 2; Video 1). The healthy volunteers were positioned supine with head and neck elevation and the arm placed along the body. The fascicles of the BP were located on an axial view at the supraclavicular notch. The US probe was translated in the transverse axial plane along a high medial to proximal axis to allow the fascicles to be analyzed, and then the trunks and roots of the BP. The “ski lift” method ends at the origin of the C5 and C6 roots where they make contact with the bifid transverse processes of the C5 and C6 vertebrae. Starting at the C7 root, the origin is located in front of the non-bifid transverse processes (Martinoli et al., 2002).

After the C5 and C6 roots were located, the BP was re-explored in the same plane but in the reverse direction (i.e. transverse axial plane and proximal-to-distal scanning). This resulted in back and forth scanning of the BP. The UTBP was located by following the C5 C6 roots to where they converge. The SSN was analyzed from its origin to its most lateral portion before it entered the scapular region. The US description consisted of the diameter (in millimeters), depth (distance of orSSN from skin in millimeters) and location of the origin (C5 root, UTBP, branches of division of UTBP).

Accuracy of Targeting the SSN with US in Cadavers

Ten SSN origins in five cadavers were explored with US and then dissected. A superficial 12-MHz transducer with a LOGIQe portable ultrasound (General Electric, Milwaukee, WI, USA) was used. US was used to mark the orSSN with a thin needle (21 G) and to inject 1 cc of methylene blue (MB) (Figs. 3 and 4).

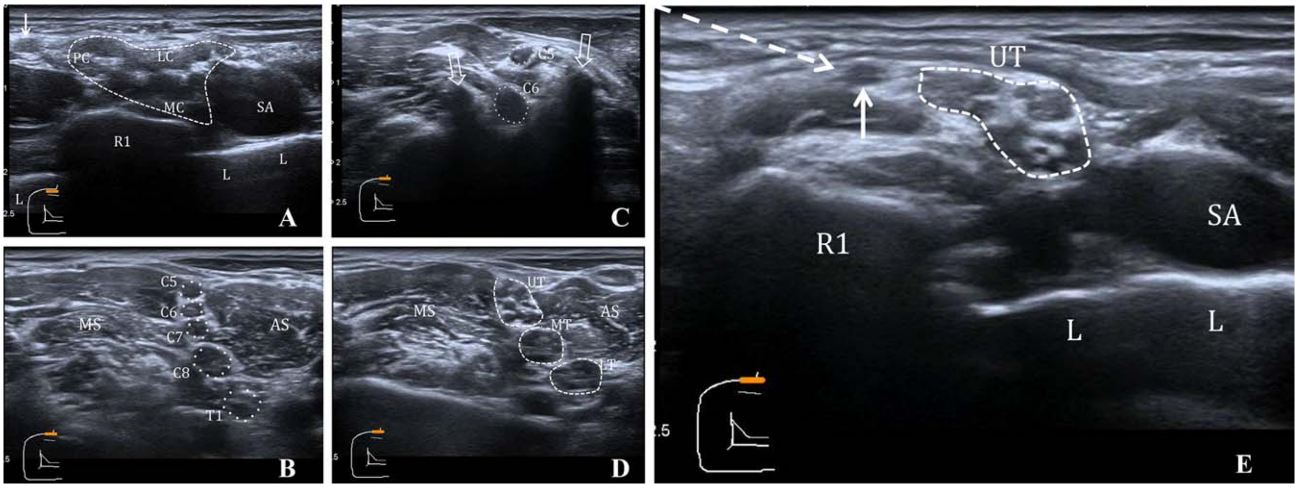

Fig. 2. Reference horizontal slices used to analyze the BP and locate the origin of the SSN. **(a)** At the supraclavicular level, fascicles from the BP bundles correspond to small, rounded hypoechogenic formations (surrounded by dashed line) located outside the SA, above the first rib (R1) and the lung apex (L, lung). The SSN (arrow) is visible outside the bundles. PC, posterior cord; LC, lateral cord; MC, medial cord. **(b)** At the interscalene triangle, the roots are superimposed (dashed lines) between the AS and the middle scalene (MS); C5 is the most superficial root. **(c)** In the periforaminal region, the contours of the contacting transverse processes where the roots pass through constitute a good US landmark. At C6 and above it, the transverse processes are bifid with one anterior and one posterior process (open arrows). **(d)** During the descent phase of the probe, the UT (dashed line) and its fascicles are located distal to the anastomosis between the C5 and C6 roots. MT, middle trunk; LT, lower trunk; MS, middle scalene; AS, anterior scalene. **(e)** Distal to the interscalene triangle, the SSN (arrow) separates itself from the superior trunk (UT) (or its posterior division). The trajectory of the needle used to mark the nerve and inject dye at the origin of the SSN is shown as a dashed line and arrow. R1, first rib; SA, subclavian artery; L, lung apex. [Color figure can be viewed at wileyonlinelibrary.com]

The cadavers were positioned supine, the arm placed along the body and the head turned to the opposite side, with no head and neck elevation. The US exploration method was the same as the one used in the healthy volunteers (Lapegue et al., 2014). After the origin of the SSN had been located, the needle was inserted parallel to the long axis of the probe until the origin was reached; this provided a lateral approach to the nerve's origin (Fig. 3).

The cadaver specimens were dissected to determine whether the SSN's anatomical origin in the limbs

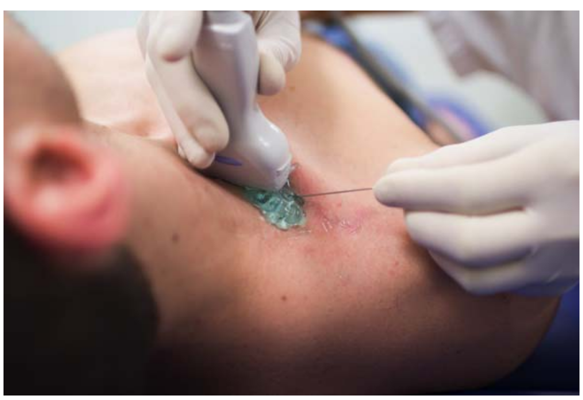

Fig. 3. Locating the origin of the SSN with ultrasound and marking with a small needle. After the back-and-forth "ski lift" maneuver, the probe was placed above the supraclavicular notch. The needle was introduced laterally along with probe's long axis through a gel pad so its trajectory to the target SSN could be followed more readily. [Color figure can be viewed at wileyonlinelibrary.com]

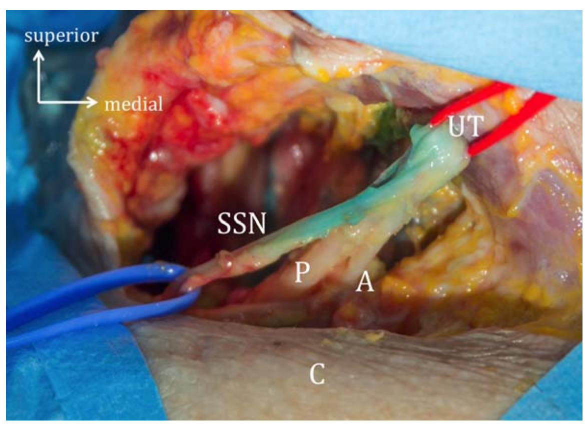

Fig. 4. Isolated marking of the origin of the SSN after ultrasound-guided injection of MB in cadaver specimen No. 1. The origin of the SSN is marked with MB. The SSN and the UT with its anterior (A) and posterior (P) divisions were surrounded by blue tape and red tape, respectively; C, clavicle. [Color figure can be viewed at wileyonlinelibrary.com]

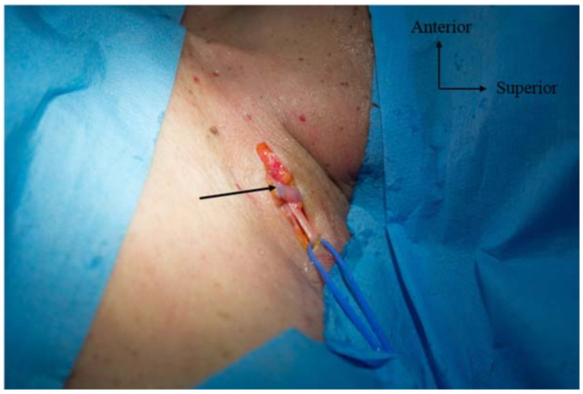

Fig. 5. Failed staining of the SSN with ultrasound on cadaver specimen No. 9. A superficial vein in the supraclavicular region (arrow) was fixed by a needle inserted under ultrasound guidance. The SSN (blue tape) is not marked. [Color figure can be viewed at wileyonlinelibrary.com]

had been marked (i.e., macroscopic origin with preservation of the mesoneurium at the orSSN). A 4-cm supraclavicular incision was made beyond the superior edge of the clavicle and the tissues were dissected to the distal end of the needle. The MB diffused after supraclavicular portion of the BP had been dissected; the mesoneurium at the orSSN was preserved during this dissection.

The following parameters were examined: fixation of the orSSN with the needle, distance (in millimeters) between the needle's tip and the orSSN measured with calipers, MB staining of the orSSN and adjacent nerve structures, location of the orSSN (i.e., UTBP, bifurcation of the UTBP, divisions of the UTBP).

Statistical analysis

Excel (Microsoft, Redmond, WA, USA) and XLSTAT 2011 (Addinsoft SARL, Paris, France) software packages were used for statistical analysis. The primary and secondary objectives were to describe the orSSN and to mark it. Results were recorded as means and minimum and maximum values. The Spearman coefficient was determined for the correlation between the SSN's depth and BMI, and between the needle/orSSN distance and BMI. Results were considered statistically significant if their P values was < 0.05.

RESULTS

US in healthy volunteers provided us with an opportunity to describe 60 proximal SSNs. The diameter of the orSSN averaged 1.33 mm (range, 1 1.9 mm) and its depth averaged 5.12 mm (range, 2.7 10.6 mm). The correlation between the SSN's depth and BMI was weak but statistically significant (r 0.499; $P < 0.05$). In subjects with a high BMI, the orSSN was not very deep (maximum of 10.6 mm) and did not hinder the analysis. The orSSN was located in the UTBP in 53 limbs and in the UTBP's posterior division in seven; the orSSN was not found at the UTBP trifurcation in any limb.

With US, the orSSN was found in nine of 10 cadaver limbs (90%) using needle fixation and MB staining (Fig. 4). In one case, a superficial supraclavicular vein was fixed and marked; the vein was injected as it passed the superior portion of the orSSN (Fig. 5).

The distance between the needle and the orSSN was 3.8 mm (range, 0 8 mm). The implanted needle was at the orSSN in two cases, proximal to it in seven (at the UTBP) and distal to it in one (superficial supraclavicular vein, Fig. 5) relative to the SSN's anatomical origin. The portion of a superficial supraclavicular vein that was fixed and stained was located on the superior edge of the UTBP. The correlation between the needle/SSN origin distance and BMI in cadavers was not significant (r 0.148; P 0.648). Only the orSSN was stained with MB in six limbs. In three cases, other

TABLE 1. Results of Targeting the Origin of the SSN with Ultrasound in Cadavers

Specimen No.	Age (years)	BMI (kg/m^2)	Needle position	SSN origin after dissection	Distance Needle/SSN origin (cm)	Staining with MB
1 (Left)	59	17	SSN origin	UTBP bifurcation	0	SSN
2 (Right)	59	17	UTBP	UTBP bifurcation	0.5	SSN
3 (Left)	85	30	UTBP	UTBP bifurcation	0.2	SSN UTBP Posterior division of UTBP
4 (Right)	85	30	UTBP	UTBP bifurcation	0.6	SSN
5 (Left)	82	25	UTBP	UTBP bifurcation	0.7	SSN UTBP
6 (Right)	82	25	UTBP	UTBP bifurcation	0.3	SSN
7 (Left)	75	25	UTBP	UTBP bifurcation	0.3	SSN
8 (Right)	75	25	SSN origin	UTBP bifurcation	0	SSN
9 (Left)	60	22	Superficial vein in supraclavicular fossa	UTBP bifurcation	0.4	Superficial vein in supraclavicular fossa
10 (Right)	60	22	UTBP	UTBP bifurcation	0.8	SSN UTBP

Abbreviations: SSN, suprascapular nerve; UTBP, upper trunk of brachial plexus.

structures were also stained: the UTBP and its posterior division (one case) or the UTBP only (two cases). After the cadaver limbs were dissected, the orSSN was identified at the bifurcation of the UTBP in all 10. The cadaver findings are summarized in Table 1.

DISCUSSION

Our primary and secondary hypotheses were confirmed. As an imaging modality, US can provide a reliable description and targeting of the orSSN, irrespective of the patient's BMI.

MRI is the gold standard for examining the BP. Nevertheless, the large field of view of MRI makes it impossible to analyze the fine nerve structures of the BP individually (Ohana et al., 2014; Marquez Neto et al., 2016). Fornage et al. (1988) showed that US was superior for studying the peripheral nervous system. The origin of the terminal branches of the PB can be determined accurately through dynamic direct exploration and the high definition of modern US machines. However, there is a long learning curve before the dynamic analysis of structures and BP anatomy can be mastered. US results are operator-dependent (Ohana et al., 2014; Tagliafico et al., 2016).

US exploration using the "ski lift" technique allowed us to describe the proximal SSN region in 100% of healthy subjects. This study found that the SSN is located superficially in the supraclavicular region; the mean distance between the SSN and the skin was 5.12 mm. The SSN's depth was weakly correlated with BMI ($P < 0.05$); however, this did not affect our ability to describe the SSN or the accuracy of targeting it with a small needle (i.e., non-significant correlation between BMI and needle/SSN origin distance). This can be explained by the superficial location of the SSN, irrespective of the subject's BMI; the depth of the orSSN ranged from 2.7 to 10.6 mm. The resolution of US images depends on the depth of the structures being analyzed (Fornage, 1988; Ohana et al., 2014). The development of high-frequency US probes has had the greatest effect on the most superficial nerves (e.g., median, radial, ulnar, and common peroneal). This study shows that the proximal portion of the SSN belongs in this superficial nerve category (Schneider-Kolsky et al., 2004; Chan and Peng, 2011; Rothe et al., 2014).

The orSSN at the level of the proximal portion of the UTBP was described by Vesalius in 1555 and Kerr in 1918 (Vesalius, 1555; Kerr, 1918; Boileau, 1972; MacKinnon and Dellon, 1988; Kline et al., 2001; Maniker, 2005; Slutsky et al., 2006; Standring, 2008; Tung and Moore, 2015; Hanna, 2016). This identified the SSN's micro-anatomical origin (i.e., SSN's fascicular origin stemming from C6, C5, or even C4) following systematic dissection of the mesoneurium (Kerr, 1918; Bonnel, 1984; Franco et al., 2008; Siqueira et al., 2010; Arad et al., 2014; Sinha et al., 2016). In more recently published studies, the SSN's anatomical origin has been found at the bifurcation of the UTBP or its posterior branch (Arad et al., 2014; Leung et al., 2014). Our dynamic US exploration method scans the BP along the length of its fascicles to determine the origin of its nerve branches; this ignores the mesoneurium and does not cause inter-fascicular dissection. However, US cannot be used to determine the exact anatomical origin of the SSN. This explains the proximal location of the orSSN at the UTBP on US in our study in 53 out of 60 (88.33%) of the healthy volunteers' limbs. We speculate that US located the orSSN near its micro-anatomical origin. This would explain why the orSSN was more proximal on US than after dissection in 70% of cases (i.e., needle positioned proximal to orSSN at the UTBP in 7 of the 10 cadaver specimens). Nevertheless, the mean distance between the needle and the SSN's anatomical origin was small: 3.8 mm (range, 0 8 mm).

SSN nerve block is the preferred treatment for addressing a wide range of chronic and acute postoperative shoulder pain conditions, such as pain after shoulder arthroscopy, trauma-induced pain, rheumatic diseases (i.e., adhesive capsulitis), and cancer (Chan and Peng, 2011). The success of ultrasound-guided SSN nerve blocks at the suprascapular notch is limited by the nerve's depth (deeper in patients with a higher BMI) and anatomical variations in the origin of the sensory branches. In 50% of cases, the origin of the sensory branches of the SSN is proximal to the suprascapular notch (Aszmann et al., 1996; Harmon and Hearty, 2007; Vorster et al., 2008; Cahn and Peng, 2011; Siegenthaler et al., 2012; Rothe et al., 2014). We speculate that US-guided supraclavicular block of the proximal SSN is a good alternative, especially in patients with a high BMI. Nevertheless, further research into the anatomical relationship between the proximal SSN and vascular structures and the phrenic nerve are needed to assess the iatrogenic risks related to injecting anesthetic products (Siegenthaler et al., 2012; Hackworth, 2013; Rothe et al., 2014). Intravenous injection occurred in one case in our study; this was an unwanted event that could be prevented by using Doppler ultrasound and looking for venous reflux before injection.

Although US is an operator-dependent modality, a single, experienced radiologist performed all the US descriptions and targeting in this study; no intra-class correlation could be calculated since there was no second series of measurements by an independent radiologist.

This study has the biases inherent in cadaver studies. The mean age of the cadavers (72.2 years) was higher than that of the healthy volunteers (33.4 years). The position of elevation of head and neck improves the ease with which the SSN can be seen (Lapegue et al., 2014); this was not possible in cadavers. Furthermore, the lack of visible blood flow during US exploration made it more challenging to describe the SSN and its surrounding vascular structures. Diffusion of MB away from the injection point did not allow for accurate assessment of the orSSN and could have led to overestimation of the number of marked nerve origins. Excessive dispersion of the staining dye increases the chance that the orSSN will be marked (i.e., multiple nerve structures stained in three cadaver limbs). The cadaver dissection step could have altered the normal anatomy and/or the needle's positioning, which could have distorted the study's findings.

CONCLUSION

US is a valid modality for describing and targeting the orSSN. A feasibility study with cadavers is needed to judge the risk/benefit balance in US-guided supraclavicular block of the proximal SSN.

ACKNOWLEDGMENTS

The authors would like to thank the persons who donated their bodies to the department of *Laboratory* of Applied *Anatomy* (Faculty of Medicine, *Toulouse, France)*, without which this study would not have been possible.

REFERENCES

Ahlawat S, Wadhwa V, Belzberg AJ, et al. 2015. Spectrum of suprascapular nerve lesions: normal and abnormal neuromuscular imaging appearances on 3-T MR neurography. Am J Roentgenol 204:589–601.

Arad E, Li Z, Sitzman TJ, et al. 2014. Anatomic sites of origin of the suprascapular and lateral pectoral nerves within the brachial plexus. Plast Reconstr Surg 133:20e–27e.

Aszmann OC, Dellon AL, Birely BT, McFarland EG. 1996. Innervation of the human shoulder joint and its implications for surgery. Clin Orthop 330:202–207.

Battaglia PJ, Haun DW, Dooley K, Kettner NW. 2014. Sonographic-measurement of the normal suprascapular nerve and omohyoid muscle. Man Ther 19:165–168.

Bharti N, Bhardawaj N, Wig J. 2015. Comparison of ultrasound-guided supraclavicular, infraclavicular and below-C6 interscalene brachial plexus block for upper limb surgery: a randomised, observer-blinded study. Anaesth Intensive Care 43:468–472.

Boileau JC. 1972. Grant 's: Atlas of Anatomy. 6th Ed. Baltimore: Williams & Wilkins. 476 p.

Bonnel F. 1984. Microscopic anatomy of the adult human brachial plexus: an anatomical and histological basis for microsurgery. Microsurgery 5:107–118.

Boykin RE, Friedman DJ, Higgins LD, Warner JJP. 2010. Suprascapular neuropathy. J Bone Joint Surg Am 92:2348–2364.

Chalian M, Faridian-Aragh N, Soldatos T, et al. 2011. High-resolution 3T MR neurography of suprascapular neuropathy. Acad Radiol 18:1049–1059.

Chan C, Peng PWH. 2011. Suprascapular nerve block: a narrative review. Reg Anesth Pain Med 36:358–373.

Chang KV, Hung CY, Wu WT, et al. 2016. Comparison of the effectiveness of suprascapular nerve block with physical therapy, placebo, and intra-articular injection in management of chronic shoulder pain: a meta-analysis of Randomized Controlled Trials. Arch Phys Med Rehabil 97:1366–1380.

Dhir S, Sondekoppam RV, Sharma R, Ganapathy S, Athwal GS. 2016. A Comparison of Combined Suprascapular and Axillary Nerve Blocks to Interscalene Nerve Block for Analgesia in Arthroscopic Shoulder Surgery: An Equivalence Study. Reg Anesth Pain Med 41:564–571.

Franco CD, Rahman A, Voronov G, et al. 2008. Gross anatomy of the brachial plexus sheath in human cadavers. Reg Anesth Pain Med 33:64–69.

Fornage BD. 1988. Peripheral nerves of the extremities: imaging with US. Radiology 167:179–182.

Hackworth RJ. 2013. A new and simplified approach to target the suprascapular nerve with ultrasound. J Clin Anesth 25:347–348.

Hanna A. 2016. The SPA arrangement of the branches of the upper trunk of the brachial plexus: a correction of a longstanding misconception and a new diagram of the brachial plexus. J Neurosurg 125: 350–354.

Harmon D, Hearty C. 2007. Ultrasound-guided suprascapular nerve block technique. Pain Phys 10:743–746.

Karataş GK, Meray J. 2002. Suprascapular nerve block for pain relief in adhesive capsulitis: comparison of 2 different techniques. Arch Phys Med Rehabil 83:593–597.

Kerr AT. 1918. The brachial plexus of nerves in man: The variations in its formation and branches. Am J Anat 23:285–395.

Kline DG, Hudson AR, Kim DH. 2001. Atlas of Peripheral Nerve Surgery. Philadelphia: Saunders. p 11–208.

Lapegue F, Faruch-Bilfeld M, Demondion X, et al. 2014. Ultrasonography of the brachial plexus, normal appearance and practical applications. Diagn Interv Imaging 95:259–275.

Leung S, Zlotolow DA, Kozin SH, Abzug JM. 2015. Surgical Anatomy of the Supraclavicular Brachial Plexus. J Bone Joint Surg Am 97: 1067–1073.

Lewis SR, Price A, Walker KJ, et al. 2015. Ultrasound guidance for upper and lower limb blocks Cochrane Database Syst Rev 9: CD006459.

MacKinnon SE, Dellon AL. 1988. Surgery of the Peripheral Nerve. 1st Ed. New York: Thieme. p 425.

Maniker AH. 2005. Operative Exposures in Peripheral Nerve Surgery. 1st Ed. New York: Thieme. p 15 .

Marquez Neto OR, Leite MS, Freitas T, et al. 2016. The role of magnetic resonance imaging in the evaluation of peripheral nerves following traumatic lesion: where do we stand? Acta Neurochir (Wien) 159:281–290.

Martinoli C, Bianchi S, Santacroce E, et al. 2002. Brachial plexus sonography: a technique for assessing the root level. Am J Roentgenol 179:699–702.

Ohana M, Moser T, Moussaouï A, et al. 2014. Current and future imaging of the peripheral nervous system. Diagn Interv Imaging 95:17–26.

Rothe C, Steen-Hansen C, Lund J, et al. 2014. Ultrasound-guided block of the suprascapular nerve - a volunteer study of a new proximal approach. Acta Anaesthesiol Scand 58:1228–1232.

Schneider-Kolsky ME, Pike J, Connell DA. 2004. CT-guided suprascapular nerve blocks: a pilot study. Skeletal Radiol 33:277–282.

Siqueira MG, Foroni LHL, Martins RS, et al. 2010. Fascicular topography of the suprascapular nerve in the C5 root and upper trunk of the brachial plexus: a microanatomic study from a nerve surgeon's perspective. Neurosurgery 67:402–406.

Siegenthaler A, Moriggl B, Mlekusch S, et al. 2012. Ultrasound-guided suprascapular nerve block, description of a novel supraclavicular approach. Reg Anesth Pain Med 37:325–328.

Sinha S, Prasad GL, Lalwani S. 2016. A cadaveric microanatomical study of the fascicular topography of the brachial plexus. J Neurosurg 125:355–362.

Slutsky DJ, Hentz VR. 2006. Peripheral Nerve Surgery: Practical Applications in the Upper Extremity. 1st Ed. Philadelphia: Churchill Livingstone Elsevier, 2006, p 97.

Stein BE, Srikumaran U, Tan EW, et al. 2012. Lower-extremity peripheral nerve blocks in the perioperative pain management of orthopaedic patients: AAOS exhibit selection. J Bone Joint Surg Am 94:e167.

Standring S. 2008. Gray's Anatomy: The Anatomical Basis of Clinical Practice. 40th Ed. London: Churchill Livingstone Elsevier. p 781–819.

Tagliafico A, Bignotti B, Martinoli C. 2016. Update on Ultrasound-Guided Interventional Procedures on Peripheral Nerves. Semin Musculoskelet Radiol 20:453–460.

Tung TH, Moore AM. 2015. Brachial plexus injuries. In: Mackinnon SE, editor: Nerve Surgery. New York: Thieme, 2015. p 393.

Vesalius A. 1555. De Humani Corporis Fabrica Libri Septem. 2nd Ed. Basel, Switzerland: Ioannem Oporinum.

Vorster W, Lange CPE, Briët RJP, et al. 2008. The sensory branch distribution of the suprascapular nerve: an anatomic study. J Shoulder Elbow Surg 17:500–502.

Wang X, Harrison C, Mariappan YK, et al. 2016. MR Neurography of Brachial Plexus at 3.0 T with Robust Fat and Blood Suppression. Radiology 152842.